Supporting information:

Insights into the structure and the electrochemical reactivity of cobalt-manganese layered double hydroxides

Hani Farhat[a], Christine Taviot-Gueho[a], Guillaume Monier[b], Valérie Briois[c], Claude Forano*[,a] and Christine Mousty*[,a]

[a] Université Clermont Auvergne, CNRS, SIGMA Clermont, Institut de Chimie de Clermont-Ferrand, F-63000 Clermont–Ferrand, France.

[b] Université Clermont Auvergne, CNRS, SIGMA Clermont, Institut Pascal, F-63000 Clermont–Ferrand, France.

[c] Synchrotron SOLEIL, CNRS-UR1, BP 48, L'orme des Merisiers, 91192 Gif-sur-Yvette, France.

Table S1. XPS peak positions of $Co2p_{3/2}$, $Mn2p_{3/2}$ and O1s in Co_RMn-LDH.

Species	Co_1Mn	Co_2Mn	Co_3Mn	Co_4Mn	Co_5Mn	Co_3Mn post CV
			E_b (eV) of $Co2p_{3/2}$			
Co(III)	780.6	780.4	780.3	780.4	780.4	780.2
	781.9	781.8	781.6	781.7	781.7	781.5
	783.6	783.4	783.3	783.4	783.4	783.2
Sat	790.6	790.4	790.3	790.4	790.4	790.2
Co(II)	780.9	780.7	780.6	780.7	780.7	
	782.7	782.5	782.4	782.5	782.5	
Sat	786.5	786.3	786.2	786.3	786.3	
			E_b (eV) of $Mn2p_{3/2}$			
Mn(II)		640.5		640.6	640.5	
		641.4		641.5	641.4	
		642.4		642.5	642.4	
		643.3		643.4	643.3	
		646.2		646.3	646.2	
Mn(III)	641.2	641.1	641.1	641.2	641.1	
	642.3	642.2	642.2	642.3	642.2	
	643.5	643.4	643.4	643.5	643.4	
	645.0	644.9	644.9	645.0	644.9	
Sat	647.0	646.9	646.9	647.0	646.9	
Mn(IV)						642.2
						643.0
						643.7
						644.5
						645.3
			E_b (eV) of O1s			
M-O	529.8	529.7	529.6	529.6	529.6	530.0
M-OH	531.2	531.2	531.2	531.2	531.2	531.2
H_2O	532.2	532.2	532.2	532.2	532.2	532.0
CO_3^{2-}	533.1	533.1	533.1	533.1	533.1	533.1
O_{2surf}	-	527.7	-	527.9	527.7	-

Table S2. Refined atomic position parameters.

Atom	Site	x	y	z	Biso ($Å^2$)	SOF (%)
Mn	3a	0	0	0	1.92(3)	24.4
Co	3a	0	0	0	1.92(3)	75.6
OH1	6c	1/3	2/3	0.04261(8)	2.47(8)	100
C	6c	0	0	1/6	3.5	5.8
O1	18g	0.087(3)	2/3	1/6	3.5	12.9
Ow	3b	1/3	2/3	1/6	3.5	30.5
OH2	6c	0	0	0.197(1)	3.5	8.5

Table S3. Refined bond distances and bond angles.

Distance (Å)		Angle (°)	
Mn/Co-OH1	2.043(1)		
OH1-OH1 out of plane	2.646(2)	OH1-Mn/Co-OH1	80.70(9)
OH1-OH1 in plane	3.11450(1)	OH1-Mn/Co-OH1	99.30(4)
C-O1	1.197(6)	O1-C-O1	120.0(4)
O1-OH1	2.928(3)		
O1-Ow	2.811(3)		
O1-OH2	3.037(11)		
OH1- Ow	2.825(2)		
OH2- Ow	3.662(6)		
OH1- Ow2	2.79(2)		

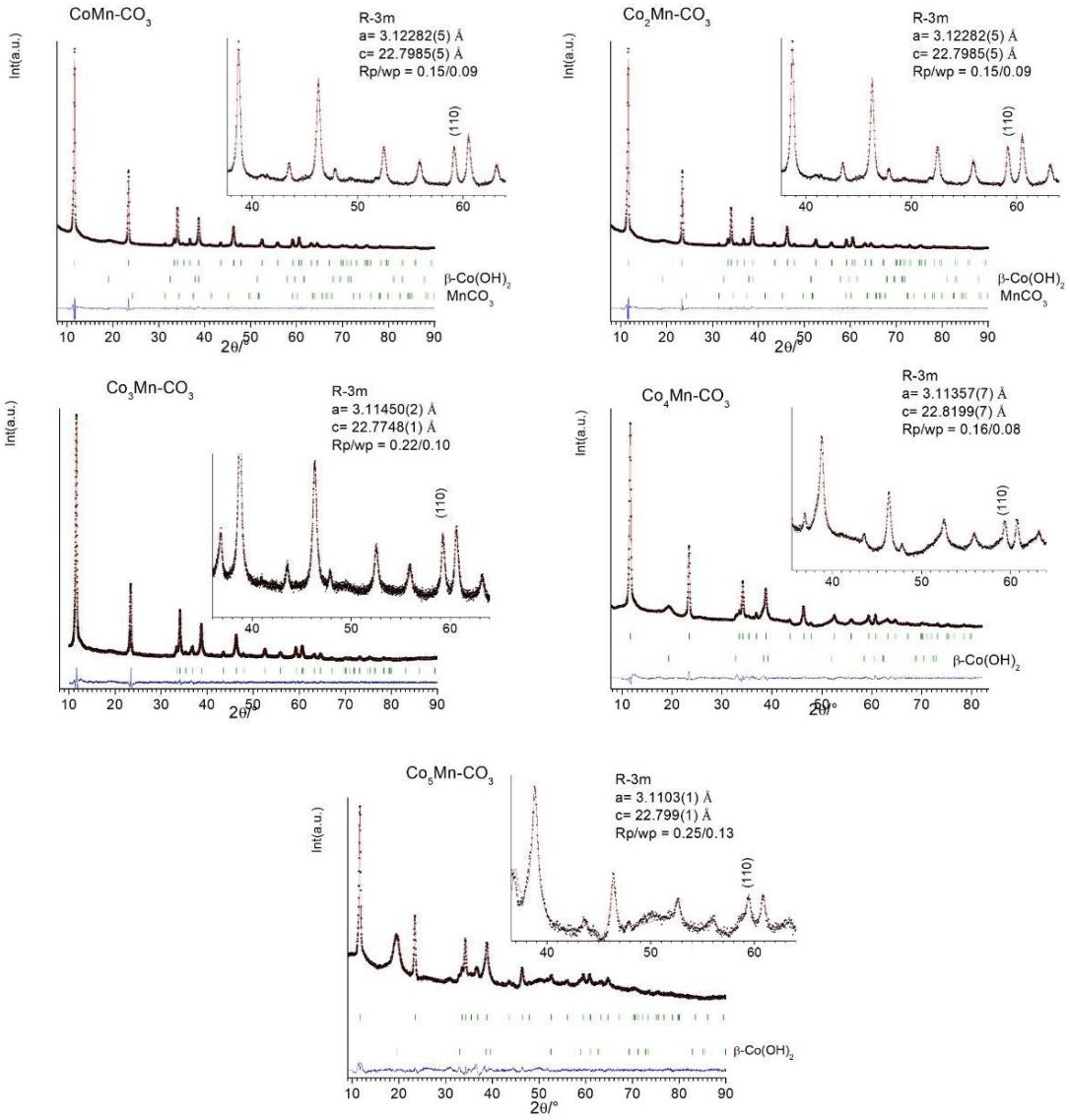

Figure S1. Profile refinement of the powder x-ray diffraction patterns of Co_RMn-LDH sample series (R=1, 2, 3, 4, 5): Experimental powder X-ray diffraction pattern (black dots), calculated pattern (solid red line), Bragg reflections (green ticks), and difference profiles (blue dots, at the bottom).

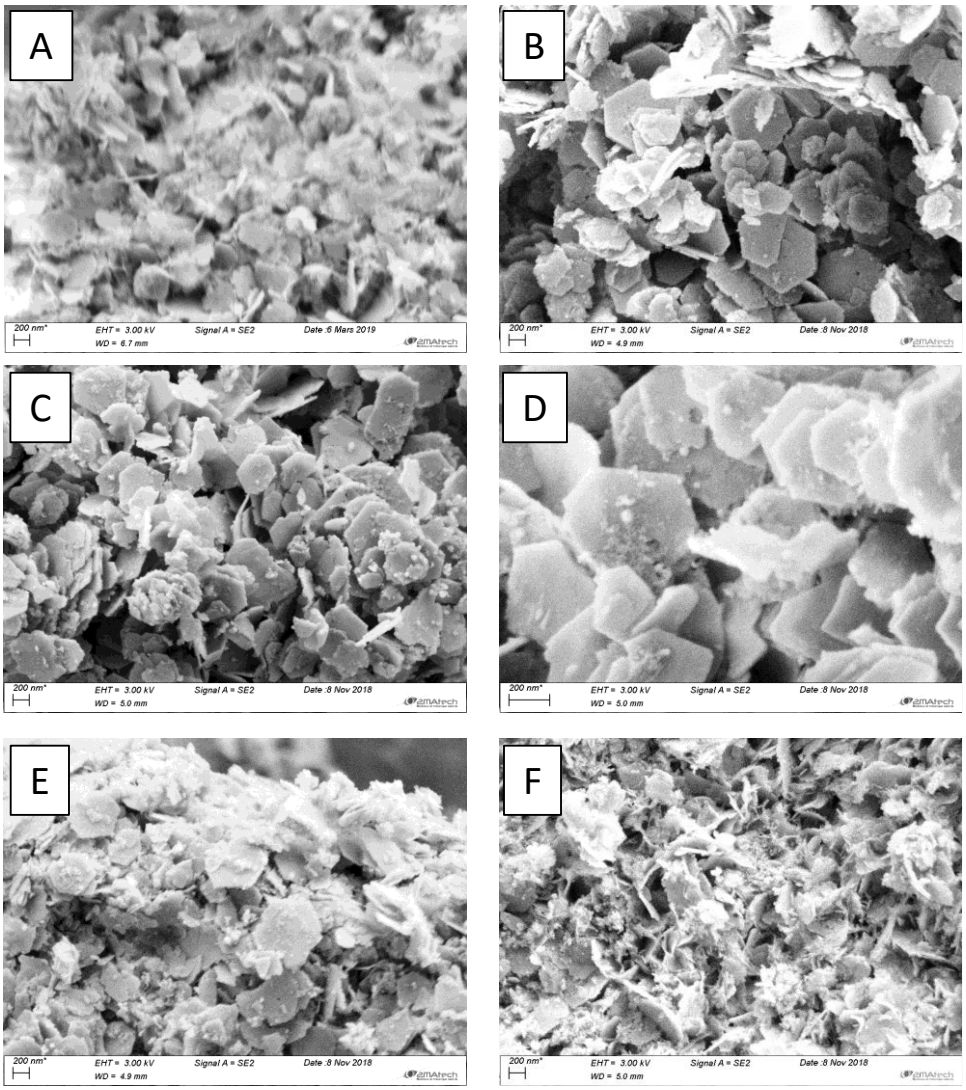

Figure S2. SEM images of A) Co_1Mn (x20 K), B) Co_2Mn (x20 K), C) Co_3Mn(x20 K), D) Co_3Mn (x50 K), E) Co_4Mn (x20 K) and F) Co_5Mn (x20 K).

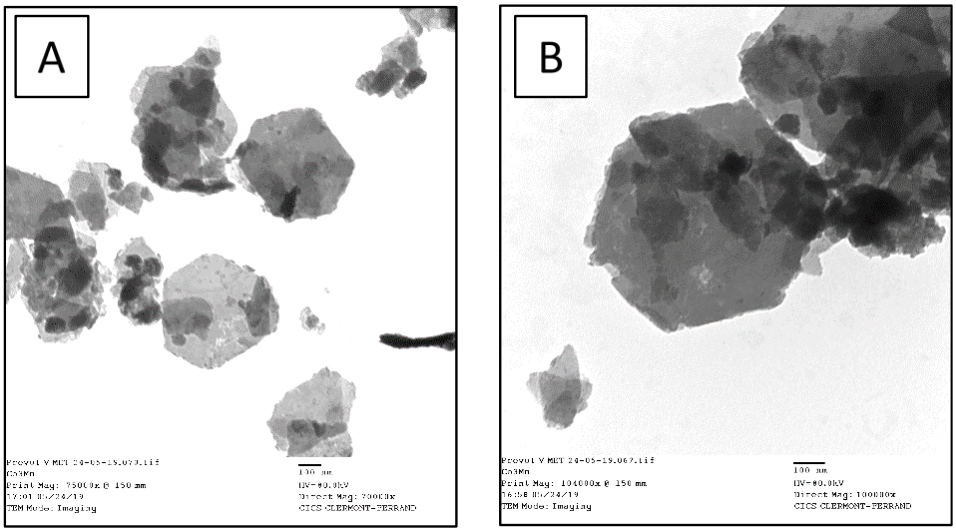

Figure S3. TEM images of Co_3Mn-LDH at **A)** 75 K and **B)** 104 K of magnification.

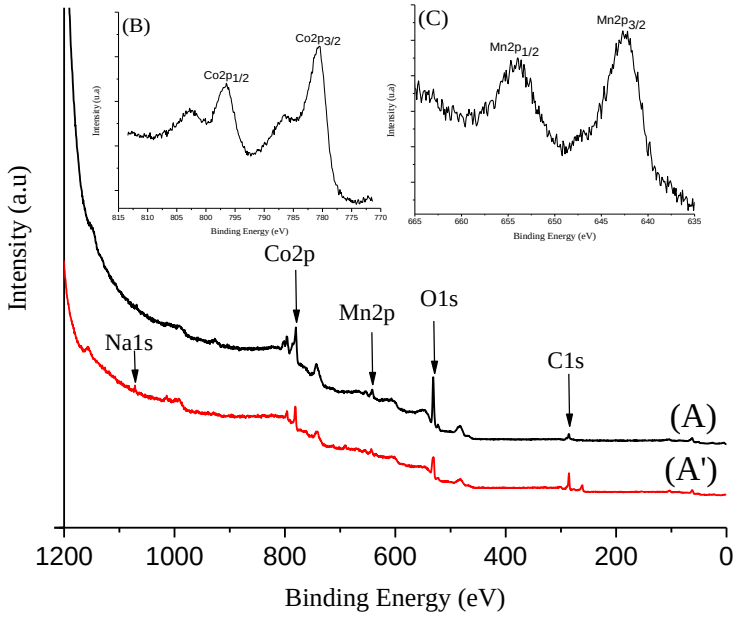

Figure S4. XPS survey spectra Co_3Mn-LDH (A) before and (A') after electrochemical oxidation. XPS spectra of Co2p (B) and Mn2p (C) in the pristine sample.

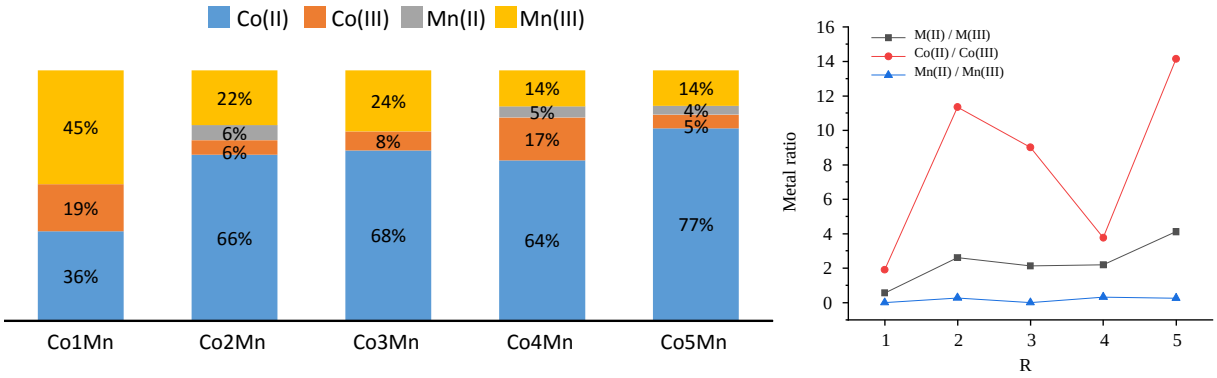

Figure S5. Evolution of **(A)** Co(II), Co(III), Mn(II) and Mn(III) percentages and **(B)** M(II)/M(III) molar ratio in the Co_RMn-LDH ($1 \leq R \leq 5$) series determined by XPS.

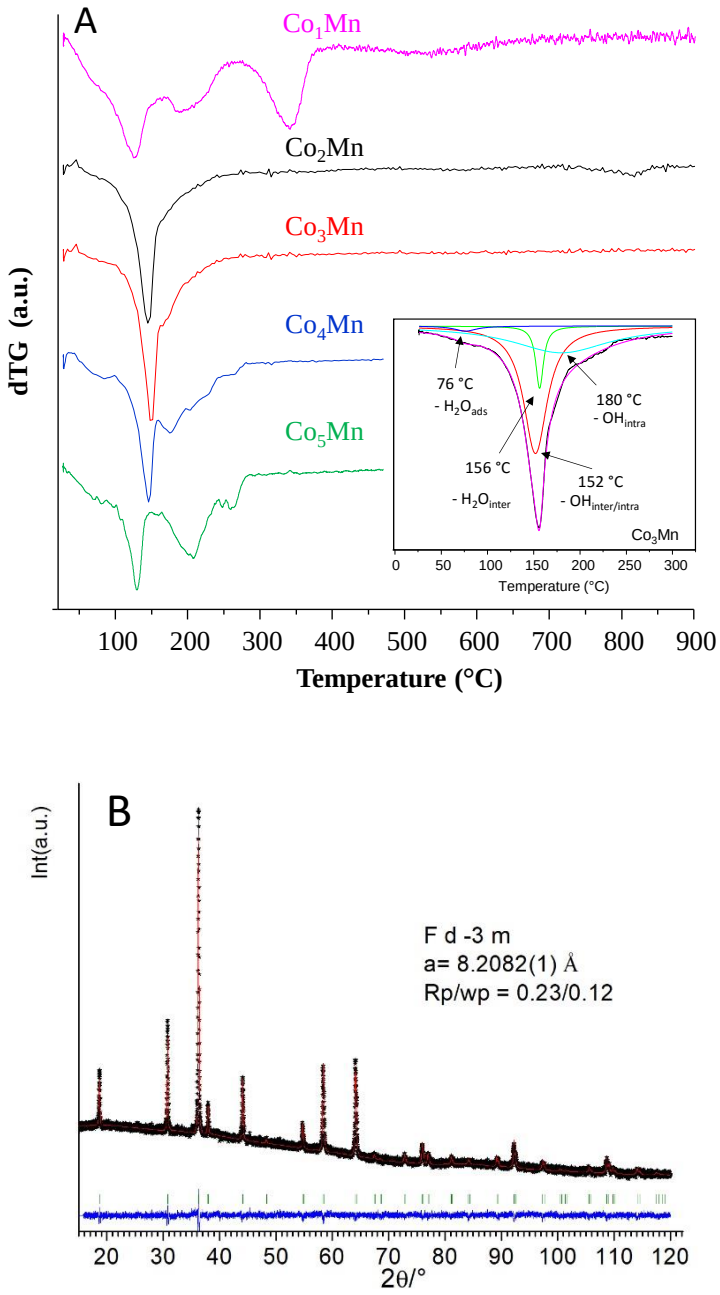

Figure S6. **A)** Differential thermogravimetric of the Co_RMn-LDH compounds. Insert shows the different dehydration events for Co_3Mn-LDH. **B)** Profile refinement of the powder x-ray diffraction pattern the TGA residue of Co_3Mn-LDH sample obtained at 900°C: Experimental powder X-ray diffraction pattern (black dots), calculated pattern (solid red line), Bragg reflections (green ticks), and difference profiles (blue dots, at the bottom).

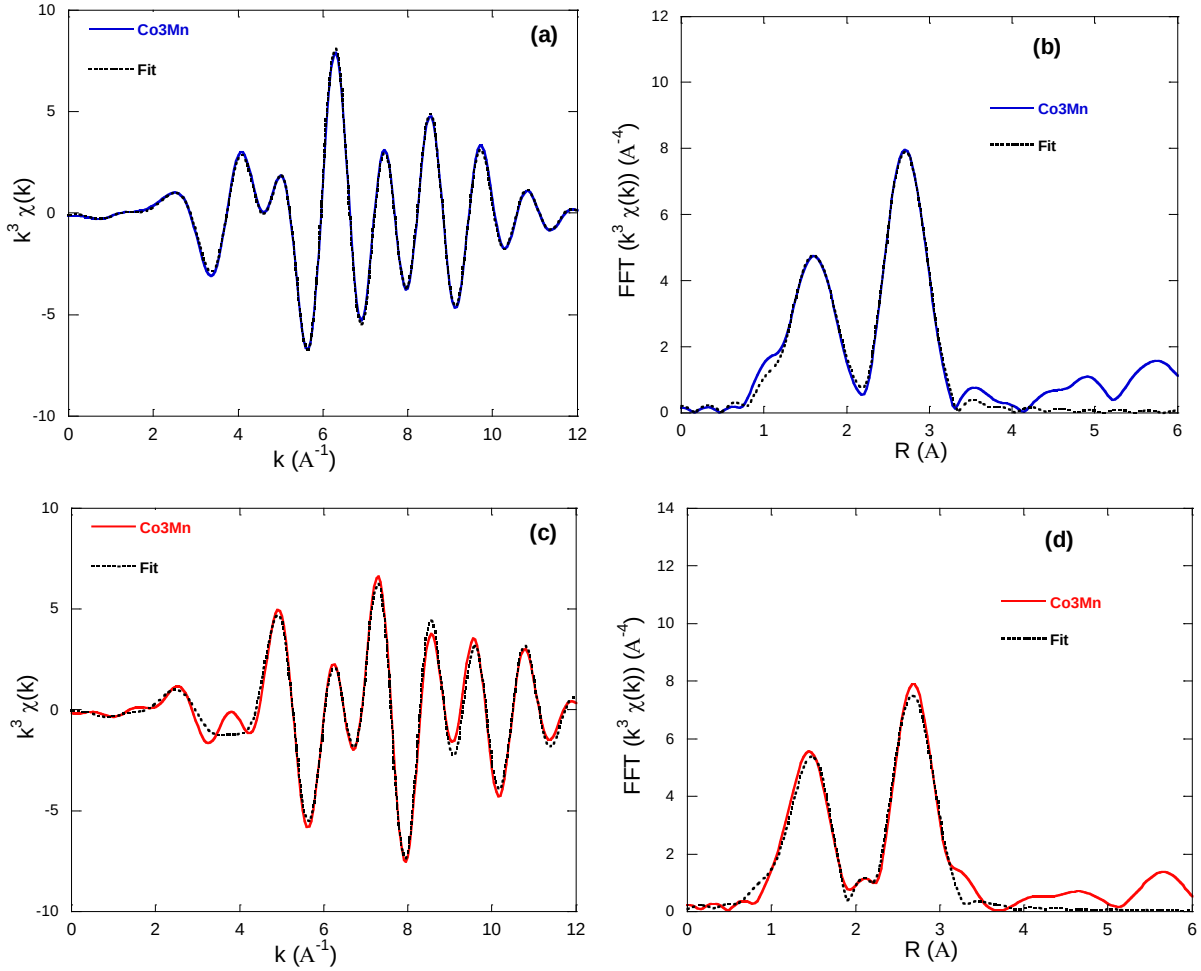

Figure S7. EXAFS data for the pristine Co_3Mn LDH showing the imaginary part of the $k^3.\chi(k)$ EXAFS signals at the Co K edge (a) and at the Mn K edge (c) and the magnitude of the k^3-weighted Fourier transforms of $\chi(k)$ at the Co K edge (b) and at the Mn K edge (d).

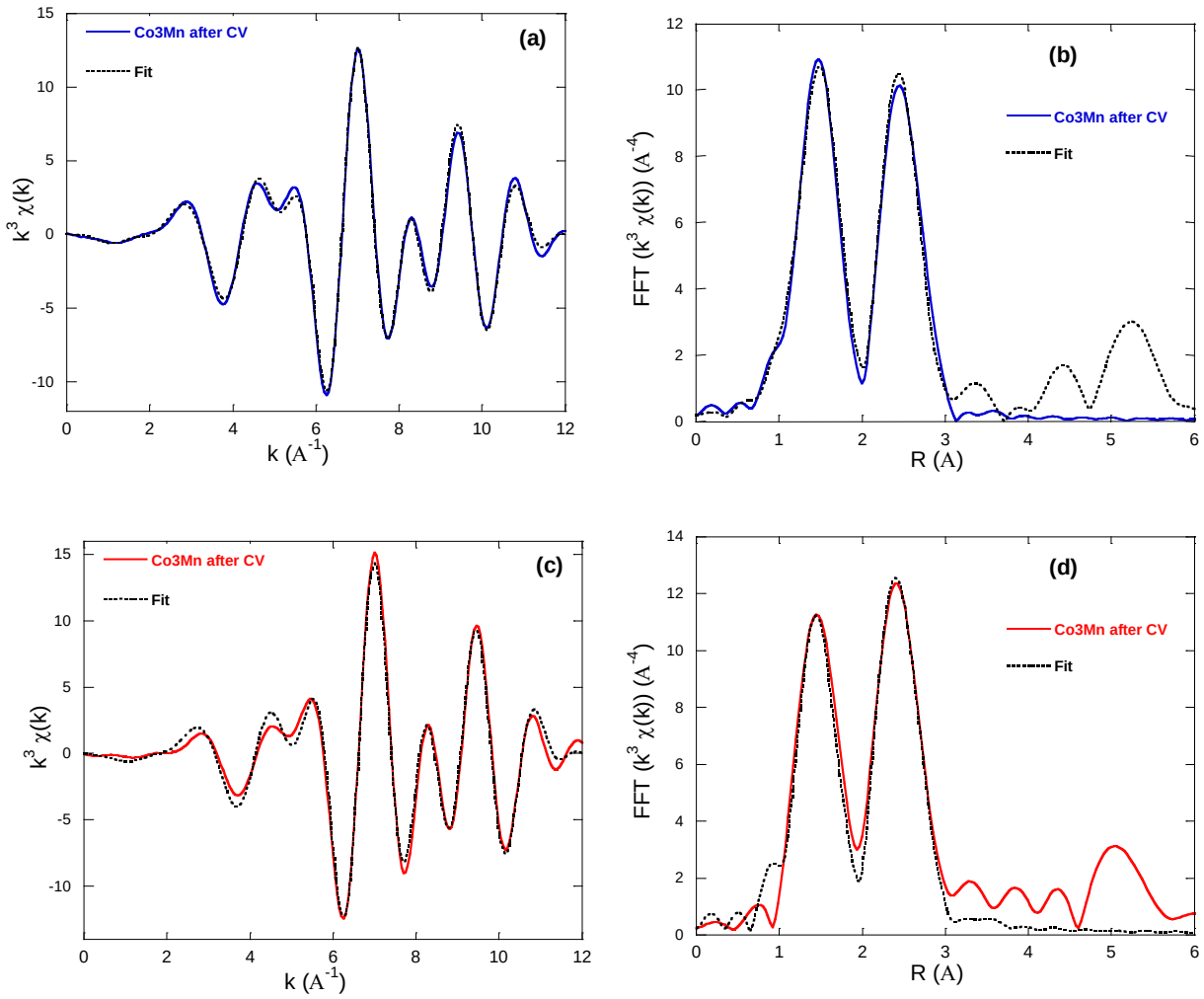

Figure S8. EXAFS data for the pristine Co_3Mn LDH after CV showing the imaginary part of the $k^3.\chi(k)$ EXAFS signals at the Co K edge (a) and at the Mn K edge (c) and the magnitude of the k^3-weighted Fourier transforms of $\chi(k)$ at the Co K edge (b) and at the Mn K edge (d).

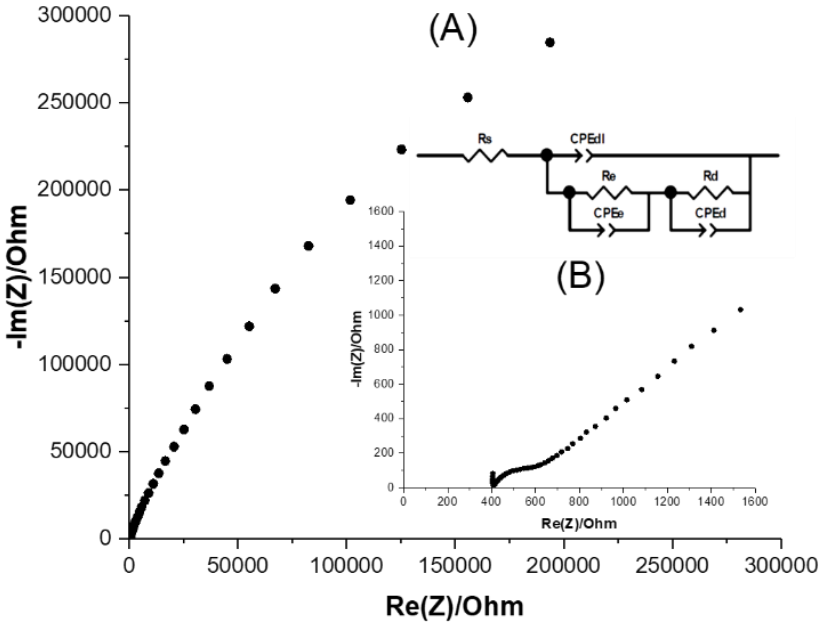

Figure S9. Nyquist plots of Co_3Mn-LDH at **A)** OCP and **B**) 0.3 V, Equivalent circuit: R_s represents the electrolyte resistance, CPE_{dl} (p_{dl} 0.9) the double layer capacitance at the interface solid/solution. R_e and CPE_e (p_e ~0.9) describe the electronic transfer resistance inside the material and a related constant phase element due to inter-granular roughness. R_d and CPE_d (p_d 0.5) represent the Warburg impedance associated to ion diffusion from the electrolyte solution within the LDH film.

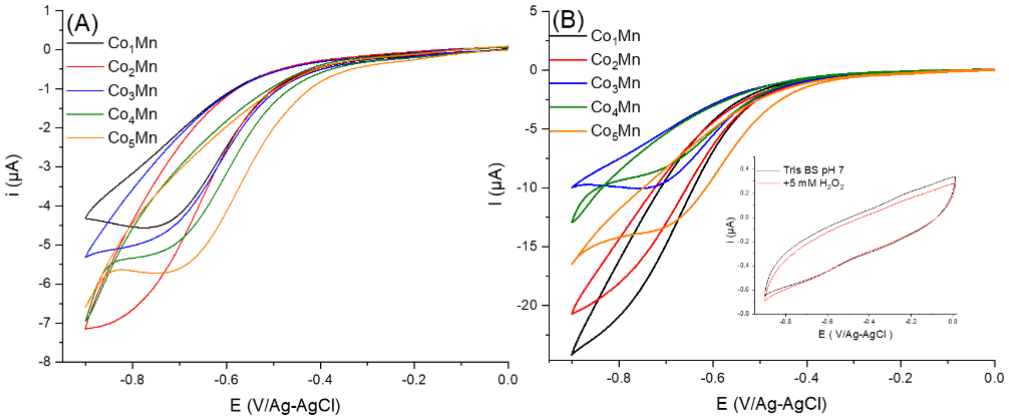

Figure S10. Cyclic voltammograms of the Co_RMn-LDH modified electrodes ($1 \leq R \leq 5$) (Cathodic sweep) in 0.1 M Tris buffer solution pH 7.0 (A) in absence and (B) presence of 5 mM H_2O_2. Inset shows the CV curves under the same conditions using a bare PGE (0.1 M pH 7.0 Tris buffer solution under Ar atmosphere, v = 10 mV s^{-1}).